China Steel Technical Report, No. 34, pp.40－45, (2021)

Effect of Ferro-Silicon Nitride Addition on Taphole Clay

CHIH-YING LIU*, CHING-HENG SHAO* and CHEN-YI CHIU**

** New Materials Research & Development Department, China Steel Corporation*
*** Ironmaking Department, Dragon Steel Corporation*

The combined effects of Fe-Si_3N_4 content and time of heat treatment on taphole clay were systematically investigated. Addition of Fe-Si_3N_4 was an effective solution to improve the corrosion resistance for taphole clay with short-term heating, which is an important factor to achieve optimum taphole length and tapping time. Under the formulation design in this study, further addition of SiC had limited enhancement on the corrosion resistance. After prolonged heat treatment, the apparent porosity increased and modulus of rupture decreased, which might affect the long-term "mushroom" (taphole clay deposit) stability. These structural changes were found closely related to the decomposition of Fe-Si_3N_4 which was triggered by long-term heat exposure. While increasing the Fe-Si_3N_4 content led to a larger degree of structural deteriorations, changing the SiC content was found to have limited effects. These findings thus revealed the possibility of tuning Fe-Si_3N_4 and SiC to attain a smooth tapping process while provide a stable "mushroom" that can withstand prolonged heat exposure and iron/slag attacks.

Keywords: Taphole clay, Blast furnace, Ferro-silicon nitride, Silicon carbide

1. INTRODUCTION

In blast furnace operations, the liquid pig iron and slag are discharged through a taphole into the runner system. At the end of each tap, the taphole is plugged by an unshaped refractory material, called taphole clay, using a mud gun. Depending on the tapping practice, the plugged taphole clay is baked and sintered for a predetermined period of time before it is drilled for the subsequent tap. It is crucial for taphole clay to have proper workability (plasticity and drillability) and good corrosion/wear resistances to achieve a smooth tapping process. Moreover, the taphole clay which is pushed into the blast furnace during taphole closure has to form a stable sedimentary deposit ("mushroom") on hearth wall near the taphole, protecting the furnace linings. The working environment within the blast furnace requires taphole clay to withstand prolonged heat exposure and iron/slag attacks.[1-2]

Taphole clay typically consists of oxide refractory materials, silicon carbide, silicon nitride materials, carbonaceous materials and binders. Similar to silicon carbide, the purpose of adding silicon nitride materials is to improve the corrosion resistance of taphole clay. Ferro-silicon nitride (Fe-Si_3N_4), a mixture of Si_3N_4 and Fe_3Si, has been recognized as a more cost-effective option among the Si_3N_4 sources. Since Si_3N_4 undergoes decomposition and carbothermal reduction at elevated temperature,[3-6] efforts have been made to elucidate the impact of heating to taphole clay at a fixed Si_3N_4 content.[7] However, the combined effects of Fe-Si_3N_4 content to the properties of taphole clay with respect to heating time have not been systematically studied.

In this work, we aimed to evaluate how Fe-Si_3N_4 content and time of heat treatment interactively affect the properties of taphole clay. Two heating times, 3hrs and 12hrs, were used to mimic the conditions of taphole clay during the tapping process and after prolonged heat exposure.

2. EXPERIMENTAL METHOD

2.1. Sample preparation

The composition design of taphole clays are listed in Table 1. Prefix F in the sample name (F15~F30) represents samples with different Fe-Si_3N_4 contents. Prefix S (S5~S20) represents samples with fixed Fe-Si_3N_4 while changing the amount of SiC.

Samples were dry mixed for 5min before kneading with coal tar at 60°C for 30min. The ratio of coal tar was adjusted to provide similar plasticity (Marshall value) for each mixture. The mixtures were molded into test bars (40mm x 40mm x 160mm) and heated at 1500°C for 3hrs or 12hrs under a reducing atmosphere.

2.2. Test methods

The phase composition was identified by X-ray diffraction. The percentage of weight loss was measured by weighing the sample before and after the heat treatment. The apparent porosity (AP) was measured following JIS

Table 1 Composition design of mixtures F15 to S20.

#	F15	F20	F25	F30	S5	S10	S15	S20
Oxide refractory materials (%)	65	60	55	50	50	45	40	35
Fe-Si_3N_4 (%)	15	20	25	30	25	25	25	25
SiC (%)	0	0	0	0	5	10	15	20
Carbonaceous materials (%)	20	20	20	20	20	20	20	20

R 2205 while modulus of rupture (MOR) was tested using an universal testing machine (JIS R 2553). The corrosion resistance was evaluated using a rotating furnace. Each set of corrosion test contained six samples which were arranged into a crucible. During the test, pig iron and blast furnace slag were introduced into the crucible and heated with a burner to 1550°C. The crucible was constantly rotating, allowing molten iron and slags to cover the sample surface. To enhance the corrosion speed, the iron and slag were replaced every half-hour for a total of six times. After the test, corrosion percentage was calculated by dividing the corroded depth I_1 with the original sample depth I_0. A smaller percentage represents better corrosion resistance.

3. RESULTS AND DISCUSSION

3.1 Effect of Fe-Si_3N_4 content and heating time on phase composition and properties of taphole clay

This section compares the properties of taphole clays with varying Fe-Si_3N_4 content (F15~F30) and heating time (3hrs and 12hrs). The suffix in the sample name represents its heating time. For instance, F15-3hr indicates the F15 sample with 3hrs of heat treatment.

Figure 1 shows the XRD patterns of F15-3hrs, F30-3hrs, F15-12hrs and F30-12hrs. For F15-3hrs and F30-3hrs, the main phases were corundum, β-Si3N4, Fe_3Si and quartz. The weak diffraction peaks around 20 degrees indicate the generation of Si_2N_2O. After heating for 12hrs, a decrease in β-Si_3N_4 and formation of β-SiC were observed. Moreover, peaks for Si_2N_2O became more pronounced, especially for the sample with high Fe-Si_3N_4 content (F30-12hrs).

The weight losses of F15-3hrs to F30-3hrs were similar despite their Fe-Si_3N_4 contents (Figure 2). After heating for 12hrs, a larger increment in weight loss was found for samples with higher Fe-Si_3N_4 contents. For F30-12hrs, weight loss increased by 4.4%, which was twice the increase for F15-12hrs (2.2%). Figure 3 shows how the apparent porosity changes with Fe-Si_3N_4 content and heating time. Longer heat treatment led to an increase of 2.2% in apparent porosity for samples with low Fe-Si_3N_4 contents (≤20%). This gap widened substantially as the Fe-Si_3N_4 content increased, reaching an increment of 8.3% as Fe-Si_3N_4 content reached 30%. Figure 4 presents the impact of Fe-Si_3N_4 content and heating time to the modulus of rupture. An increase of Fe-Si_3N_4 from 15% to 30% led to a slight increase in the modulus of rupture (0.9 Mpa) for samples with short-term heating. After a slight decrease (0.1 Mpa) due to

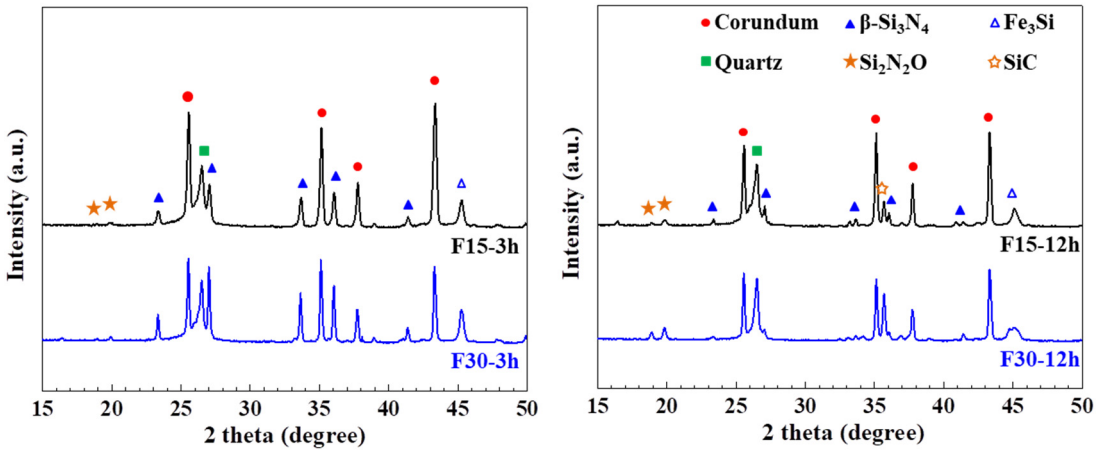

Fig.1. XRD patterns of F15-3hrs, F30-3hrs, F15-12hrs and F30-12hrs.

long-term heating for sample with 15% of Fe-Si_3N_4, larger reduction in modulus of rupture was observed for samples with higher Fe-Si_3N_4 contents. The reduction reached 4.6 Mpa as Fe-Si_3N_4 content increased to 30%.

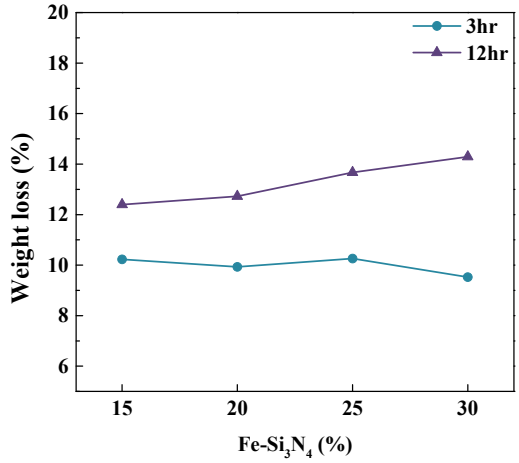

Fig.2. Changes in weight loss with respect to Fe-Si_3N_4 content and heat treatment.

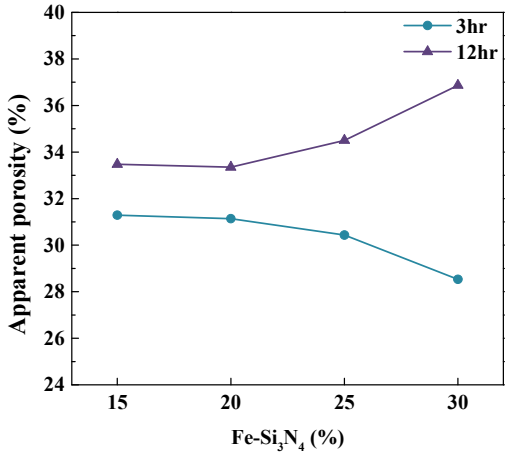

Fig.3. Changes in apparent porosity with respect to Fe-Si_3N_4 content and heat treatment.

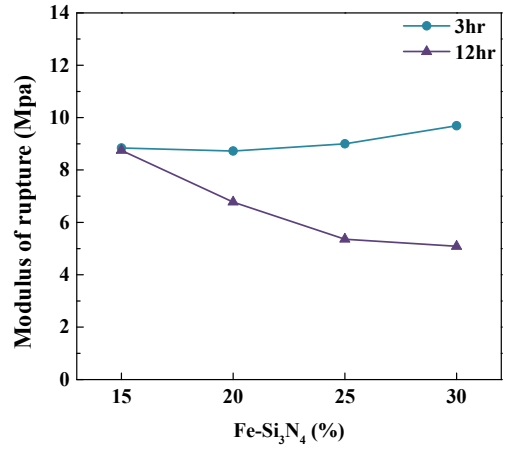

Fig.4. Changes in modulus of rupture with respect to Fe-Si_3N_4 content and heat treatment.

Figure 5 compares the corrosion indices of samples with different Fe-Si_3N_4 content and heating time. Corrosion indices for samples with the same heating time were normalized by the corrosion percentage of F15. For example, the indices of F15-3hr to F30-3hr were normalized by the corrosion percentage of F15-3hrs. A smaller index indicates a better corrosion resistance. For samples with short heat treatment, the corrosion resistance varied with its Fe-Si_3N_4 content. The corrosion index showed about 18% of improvement as Fe-Si_3N_4 content increased from 15% to 25%. After prolonged heating, the improvement via the addition of Fe-Si_3N_4 reduced to 7%.

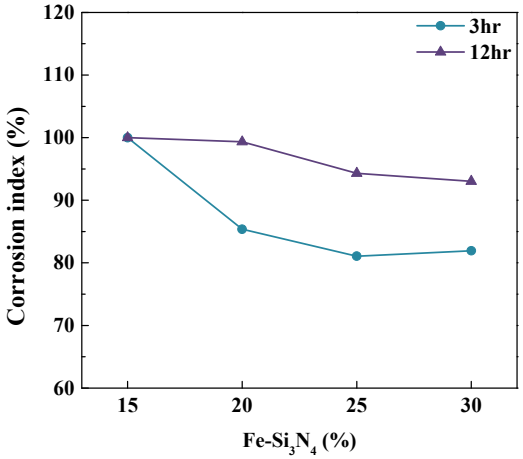

Fig.5. Changes in corrosion index with respect to Fe-Si_3N_4 content and heat treatment. The indices of samples with 3hrs of heating were normalized to the corrosion resistance of F15-3hrs while that of samples with 12hrs of heating normalized to F15-12hrs.

3.2 Effect of SiC addition on the properties of taphole clay with fixed Fe-Si_3N_4 content

This section compares the properties of taphole clays with varying SiC contents while fixing Fe-Si_3N_4 at 25%.

Weight losses of S5 to S20 with the same heat treatment were similar (Figure 6). Increasing heating time from 3hrs to 12hrs led to 4% of weight loss. Figure 7 shows how SiC content and heating time change the apparent porosity. For samples with 3hr of heating, the apparent porosity increased by 2.4% when SiC content increased from 5% to 20%. Similar trend was found for samples with 12hrs of heating. Figure 8 presents the effect of SiC content and heating time on modulus of rupture. The modulus of rupture decreased progressively from 9.5 Mpa for S5-3hrs to 6.4 Mpa for S15-3hrs, and reached 6.1 Mpa for S20-3hrs. After heating for 12hrs, moduli of rupture decreased to 5~6 Mpa for all samples.

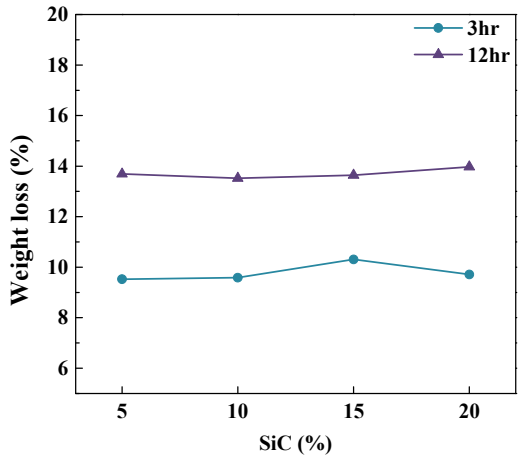

Fig.6. Changes in weight loss with respect to SiC content and heat treatment.

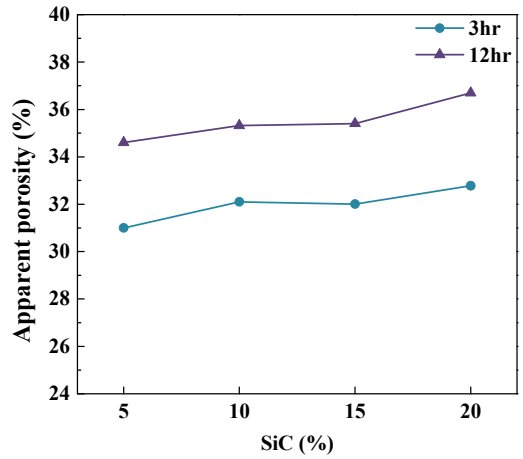

Fig.7. Changes in apparent porosity with respect to SiC content and heat treatment.

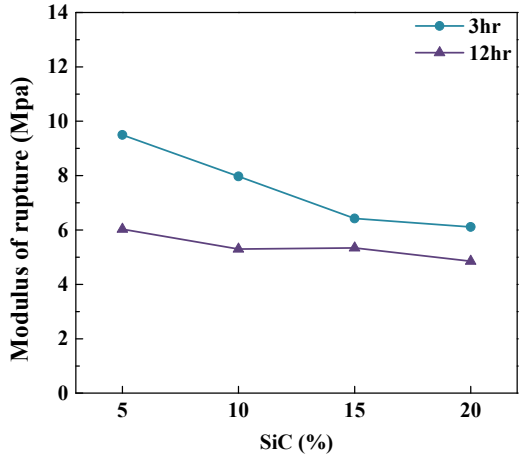

Fig.8. Changes in modulus of rupture with respect to SiC content and heat treatment.

It was found that the change in SiC content led to an initial decrease of 38% in modulus of rupture for S5 to 18% for S20 due to prolonged heat treatment.

Figure 9 compares the corrosion indices of S5 to S20 with different heating time. Corrosion indices for samples with the same heating time were normalized by the corrosion percentage of S5. For example, the indices of S10-3hrs to S20-3hrs were normalized by the corrosion percentage of S5-3hrs. With 3hrs of heat treatment, the corrosion index showed only 3% of improvement as SiC content increased from 5% to 20%. After prolonged heating, the improvement via the addition of SiC increased to 6%.

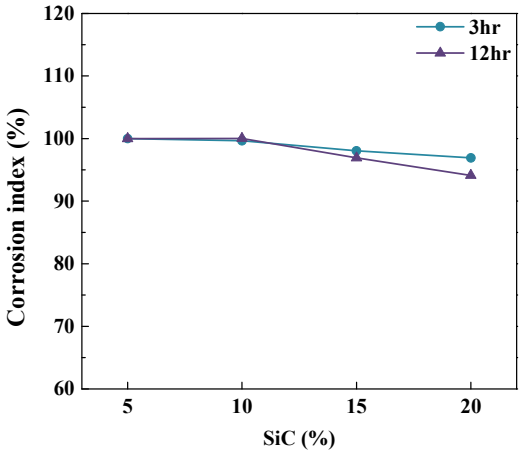

Fig.9. Changes in corrosion resistance with respect to SiC content and heat treatment. The indices of samples with 3hrs of heating were normalized to the corrosion resistance of S5-3hrs while that of samples with 12hrs of heating normalized to S5-12hrs.

3.3 Discussion

Ferrosilicon nitride is a mixture of Si_3N_4 and Fe_3Si. It is known that Si_3N_4 decomposes to Si and N_2 gas when temperature exceeds 1300°C. Meanwhile, the Fe_3Si melts around 1350°C and is found to accelerate the decomposition of Si_3N_4. In the presence of carbon source, the Si further forms SiC via a carbothermal reduction process, which becomes thermodynamically favorable when the temperature exceeds the melting point of Si (1410°C). Besides the formation of SiC, Si_2N_2O can be generated by the oxidation of Si_3N_4 at high temperature under a reducing atmosphere.[4-6]

$$Si_3N_{4(s)} \rightarrow 3Si_{(s,l)} + 2N_{2(g)}$$

$$Si_{(l)} + C_{(s)} \rightarrow SiC_{(s)}$$

$$2Si_3N_{4(s)} + 2CO_{(g)} \rightarrow 2Si_2N_2O_{(s)} + 2SiC_{(s)} + 2N_{2(g)}$$

For F15-3hrs and F30-3hrs, the SiC phase was not detected (Figure 1). Only a slight amount of Si_2N_2O was formed. After heating for 12hrs, the Si_3N_4 content decreased significantly while SiC (major) and Si_2N_2O (minor) were generated. The XRD results thus revealed that long-term heating was an important factor to the reactions of Fe-Si_3N_4 in taphole clays.

The thermal-triggered reactions of Fe-Si_3N_4 led to a series of changes in chemical and physical properties as well as the corrosion resistance of taphole clay. The weight losses of samples with 3hrs of heating were similar (~10%) regardless of their Fe-Si_3N_4 and SiC contents (Figure 2, Figure 6). This indicates that the weight change of sample with short-term heating was mainly from the loss of volatile components in coal tar. After 12hrs of heat treatment, samples with higher Fe-Si_3N_4 contents had larger weight losses. This could be attributed to the release of $N_{2(g)}$ from the decomposition of Fe-Si_3N_4 during the heating process. The change in weight loss was consistent with the XRD finding in which heating time was a crucial factor for the reactions of Fe-Si_3N_4 in taphole clays.

After short-term heating, an increase in Fe-Si_3N_4 content lowered the apparent porosity while increasing SiC led to a higher porosity (Figure 3, Figure 7). During the heat treatment at 1500°C, the Fe_3Si melted and blocked some open pores, densifying the structure of samples with high Fe-Si_3N_4. On the other hand, samples with larger SiC had poorer sinterability, resulting in larger apparent porosities. After long-term heating, the apparent porosity increased due to the release of $N_{2(g)}$ and the increment was determined by the Fe-Si_3N_4 content.

The structural densification of samples with high Fe-Si_3N_4 under short-term heating led to a slight increase in the modulus of rupture (Figure 4). On the other hand, increase in SiC content reduced the sinterability of taphole clays, hence reducing the modulus of rupture (Figure 8). After long-term heating, the modulus of rupture was found to be affected by the structural change which was caused by the decomposition of Fe-Si_3N_4. A larger starting Fe-Si_3N_4 content resulted in a higher loss of $N_{2(g)}$, leading to a larger reduction in modulus of rupture.

The corrosion resistance of taphole clay with short-term heating was significantly improved by the addition of Fe-Si_3N_4, reaching a plateau when Fe-Si_3N_4 increased to 25% (Figure 5). This could be attributed to the increase in the slag-resistant Si_3N_4 as well as the generation of Si_2N_2O.[3] After 12hrs of heat treatment, samples with higher Fe-Si_3N_4 contents generated more SiC and Si_2N_2O, which should have further improved the corrosion resistance. However, due to the increase in apparent porosity, the improvement due to the addition of Fe-Si_3N_4 after long-term heating (~7%) was not as significant as that of the samples with short-term heating (~18%). Comparing to the improvement by Fe-Si_3N_4, the effect of SiC addition (5% to 20%) to the corrosion resistance was limited (Figure 9).

Based on the above findings, it was concluded that Fe-Si_3N_4 addition significantly improved the corrosion resistance of taphole clay, especially during the first few hours of service, which is important for providing optimum taphole length and tapping time. Under the scoop of this study, the improvement reached a plateau when Fe-Si_3N_4 content increased to 25%. Addition of SiC also enhanced the corrosion resistance of taphole clay. However, the improvement under the explored SiC ratios was not as significant as that of the Fe-Si_3N_4.

Long-term heat treatment caused an increase in apparent porosity and a reduction of the modulus of rupture. These structural changes could lead to poor wear resistance as the service time of taphole clay gets longer, challenging the development of a stable "mushroom". Through the formulation design in this study, the degrees of changes in physical properties due to long-term heating were found closely related to the Fe-Si_3N_4 content. Moreover, while the limited effects on the physical properties after prolonged heating, increasing the SiC content led to a decrease in modulus of rupture for taphole clay with short-term heating. Therefore, the SiC can be used to tune the modulus of rupture to provide suitable drillability at the beginning of each tap without leading to severe degradation in wear resistance during prolonged service at high temperature.

4. CONCLUSIONS

This work demonstrated the combined effects of Fe-Si_3N_4 content and heating time on taphole clay. Two different heating times were used to mimic the conditions of taphole clay during different stages of its service life. Addition of Fe-Si_3N_4 was an effective solution to improve corrosion resistance of taphole clay with short-term heating, which is one of the important factors to achieve proper taphole length and tapping time. However, the decomposition of Fe-Si_3N_4 which was triggered by prolonged heat exposure increased the apparent porosity and reduced the modulus of rupture, potentially affecting the long-term "mushroom" stability. Under the formulation design in this study, these structural deteriorations became severer as the Fe-Si_3N_4 content increased. At fixed Fe-Si_3N_4 content, further addition of SiC also enhanced the corrosion resistance of taphole clay. Even though the improvement was not as significant as that of the Fe-Si_3N_4, addition of SiC had limited effect on the degrees of structural changes after long-term heat treatment. These findings thus revealed that taphole clay with optimum tapping performances and stable structural integrities after prolonged heat exposure can be achieved via tuning the addition of Fe-Si_3N_4 and SiC.

REFERENCE

1. L.R. Nelson and R.J. Hundermark, The tap-hole-key to furnace performance, Journal of the Southern African Institute of Mining and Metallurgy, 2016, vol. 116, pp. 465-490.
2. Y. Tang, B. Ma and Z. Gao, Latest research progress of taphole clay for blast furnaces, Refractories, 2020, vol. 54, pp. 452-456.
3. Y. Xu, Research progress of ferro-silicon nitride and its application in refractories, Refractories, 2015, vol. 49, pp. 306-312.
4. H. Wang and G S. Fischman, In situ synthesis of silicon carbide whiskers from silicon nitride powders, Journal of the American Ceramic Society, 1991, vol. 74, pp. 1519-1522.
5. H. Wang, Y. Berta, and G. S. Fischman Microstructure of silicon carbide whiskers synthesized by carbothermal reduction of silicon nitride, Journal of the American Ceramic Society, 1992, vol. 75, pp. 1080-1084.
6. H. Qin, Y. Li, X. Nie, M. Yan, P. Jiang, W. Xue, Combined effect of Fe-Si alloys and carbon on Si_3N_4 stability at elevated temperatures, Ceramics International, 2019, vol. 45, pp. 3290-3296.
7. D. Tanaka, T. Kageyama, A. Kajitani and Y. Yamamoto, Influence of Al_2O_3 fine powder addition on taphole mix property after long-time heating, Shinagawa Technical Report, 2019, vol. 62, pp. 50-62.
8. T. B. Massalski, H. Okamoto, P. R. Subramanian, and L.Kacprzak, Binary Alloy Phase Diagrams, 2nd ed., ASM International, 1990.